HHS Public Access

Author manuscript

J Bone Miner Res. Author manuscript; available in PMC 2018 May 01.

Published in final edited form as:

J Bone Miner Res. 2017 May ; 32(5): 1014–1026. doi:10.1002/jbmr.3084.

Adaptations in the Microarchitecture and Load Distribution of Maternal Cortical and Trabecular Bone in Response to Multiple Reproductive Cycles in Rats

Chantal M. J. de Bakker[1], **Allison R. Altman-Singles**[1,2], **Yihan Li**[1], **Wei-Ju Tseng**[1], **Connie Li**[1], and **X. Sherry Liu**[1,*]

Chantal M. J. de Bakker: chantald@seas.upenn.edu; Allison R. Altman-Singles: ara5093@psu.edu; Yihan Li: yihanl@seas.upenn.edu; Wei-Ju Tseng: weits@mail.med.upenn.edu; Connie Li: connie1@seas.upenn.edu

[1]McKay Orthopaedic Research Laboratory, Department of Orthopaedic Surgery, Perelman School of Medicine, University of Pennsylvania, Philadelphia, PA, United States

[2]Pennsylvania State University, Berks Campus, Reading, PA, United States

Abstract

Pregnancy, lactation, and weaning result in dramatic changes in maternal calcium metabolism. In particular, the increased calcium demand during lactation causes a substantial degree of maternal bone loss. This reproductive bone loss has been suggested to be largely reversible, as multiple clinical studies have found that parity and lactation history have no adverse effect on post-menopausal fracture risk. However, the precise effects of pregnancy, lactation, and post-weaning recovery on maternal bone structure are not well understood. Our study aimed to address this question by longitudinally tracking changes in trabecular and cortical bone microarchitecture at the proximal tibia in rats throughout three cycles of pregnancy, lactation, and post-weaning using *in vivo* μCT. We found that the trabecular thickness underwent a reversible deterioration during pregnancy and lactation, which was fully recovered after weaning, while other parameters of trabecular microarchitecture (including trabecular number, spacing, connectivity density, and structure model index) underwent a more permanent deterioration which recovered minimally. Thus, pregnancy and lactation resulted in both transient and long-lasting alterations in trabecular microstructure. In the meantime, multiple reproductive cycles appeared to improve the robustness of cortical bone (resulting in an elevated cortical area and polar moment of inertia), as well as increase the proportion of the total load carried by the cortical bone at the proximal tibia. Taken together, changes in the cortical and trabecular compartments suggest that while rat tibial trabecular bone appears to be highly involved in maintaining calcium homeostasis during female reproduction, cortical bone adapts to increase its load-bearing capacity, allowing the overall mechanical function of the tibia to be maintained.

[*]To whom correspondence should be addressed: X. Sherry Liu, McKay Orthopaedic Research Laboratory, Department of Orthopaedic Surgery, University of Pennsylvania, 426C Stemmler Hall, 36th Street and Hamilton Walk, Philadelphia, PA 19104, USA, xiaoweil@mail.med.upenn.edu, Phone: 1-215-746-4668.

Conflict of Interest:

The authors declare that they have no conflict of interest.

Keywords

pregnancy; lactation; weaning; bone microarchitecture; stiffness; bone formation

1. Introduction

The fetal/infant bone growth that takes place during pregnancy and lactation causes significant changes in maternal calcium metabolism. This increased calcium demand is partially compensated by modified intestinal absorption and renal excretion. In particular, reports have indicated that during pregnancy the fetal calcium demand is largely met through a doubling of the intestinal absorption of calcium (1,2). However, despite these compensations, the maternal skeleton also forms an important source of calcium and therefore undergoes substantial bone loss during reproduction. Clinical studies have indicated small but significant reductions in bone mass following pregnancy, although the extent of pregnancy-related bone loss in women appears to be variable and may be dependent on dietary calcium intake (2,3). On the other hand, lactation induces dramatic bone loss, as the skeleton forms the main source of calcium during lactation (1,2). Over a 6-month lactation period, women have been found to lose up to 5–7% of their bone mass (4,5), while rodents lose as much as 30% of bone mass during 3 weeks of lactation (6–8).

This reproductive bone loss undergoes a period of recovery following weaning. Rodent studies have indicated osteoclast apoptosis within 24–48 hours after weaning (9,10), which is accompanied by an increase in osteoblastic bone formation, as measured through dynamic histomorphometry (11–13). Additionally, recent studies have indicated that through reversible remodeling of the perilacunar spaces, osteocytes may also play a role in reproductive bone loss and recovery (14). Taken together, these post-weaning changes lead to a rapid accrual of bone, allowing reproductive bone loss to be largely recovered. Four weeks post-weaning, studies have shown a complete recovery of bone mass at the lumbar vertebra and a partial recovery at the tibia and femur in mice (6), thus indicating that the extent of reproductive bone loss and recovery may differ depending on the skeletal site (2,6).

Due to limitations with radiation exposure during pregnancy as well as difficulty in obtaining baseline scans in young, healthy women, few clinical studies have been able to precisely track the extent of bone recovery post-reproduction. A large number of studies have been performed that demonstrate no adverse effects of reproductive history on postmenopausal risk of fracture (15–21), and as a result of this, it is widely concluded that the effects of pregnancy and lactation are largely transient and that reproduction has minimal long-term adverse effects on bone strength or quality (2) However, to our knowledge there have been few longitudinal studies tracking the effects of reproduction on bone microstructure, and therefore the precise effects of pregnancy, lactation, and recovery post-weaning on bone structure are not well understood. Our study aimed to address this question by longitudinally tracking changes in trabecular bone microarchitecture and cortical bone structure at the proximal tibia in rats through multiple reproductive cycles using *in vivo* μCT.

Based on the wide consensus in the literature that reproductive bone loss is at most a transient process which induces no long-term, adverse effects on bone health (2,15–21), we

initially hypothesized that reproduction would result in reversible trabecular bone loss, which would be fully recovered following weaning. Thus, our first objective was to assess the precise changes in trabecular microarchitecture occurring at the proximal tibia throughout one cycle of pregnancy, lactation, and weaning with high spatial and temporal resolution. Results of this investigation indicated a dramatic extent of lactation-associated bone loss, with a much lower rate of post-weaning recovery than expected. Because the female skeleton in many cases is able to withstand the metabolic challenges associated with not just one, but multiple cycles of pregnancy and lactation with no long-term adverse consequences (16,22), we next asked the question of how the skeleton, which is substantially altered following the first reproductive cycle, would respond to subsequent cycles of pregnancy and lactation. A recent clinical study suggested that a longer duration of lactation may result in a greater cross-sectional moment of inertia at the tibia (23). Thus, we hypothesized that cortical bone adaptations may be able to compensate for trabecular bone loss, allowing the overall mechanical function of the bone to be maintained. In the second portion of the study, we investigated the impact of three consecutive cycles of pregnancy, lactation, and weaning on maternal trabecular bone as well as cortical bone structure and FEA-derived whole bone stiffness at the tibia. Overall, results of this study suggest that while rat tibial trabecular bone plays a more important role in calcium homeostasis during female reproduction, cortical bone adapts to provide greater load-bearing capacity in order to maintain the overall mechanical function of the tibia.

2. Methods

2.1 Animal Protocol

All animal procedures were reviewed and approved by the University of Pennsylvania's Institutional Animal Care and Use Committee. 24 female Sprague Dawley rats were purchased (Charles River) and allowed to acclimate for 1 month, until age 4–5 months. This age was chosen as the starting point of the experiment, as 4–5 month-old rats accurately model young adult bone, and undergo sufficiently low rates of longitudinal growth to allow precise tracking of trabecular and cortical bone structure (24). Rats were randomly assigned to 2 groups (n=12/group): reproductive and virgin. Reproductive rats underwent three complete reproductive cycles (first cycle: weeks 0–12 of the experiment, second cycle: weeks 12–21, third cycle: weeks 21–33). At week 0, rats were mated, and underwent a 3-week pregnancy, followed by a 3-week lactation period. To ensure consistent suckling intensity, litter sizes were normalized to 8–9 pups/mother within 48 hours after birth. After weaning, all rats were allowed to recover for at least 6 weeks. Rats were then mated again, and underwent two subsequent cycles of pregnancy, lactation, and post-weaning recovery. During the second reproductive cycle, rats were allowed a 3-week post-weaning recovery period, as the greatest extent of recovery was found to take place during the first three weeks post-weaning. After the third cycle, rats underwent a 6-week recovery period. Two rats failed to become pregnant during the first reproductive cycle, and one rat died during the *in vivo* scan made at the end of the third lactation period (week 27), resulting in a final sample size of n=10 for all scans up to week 27 and n=9 for weeks 30 and 33 for the reproductive group. After completing 3 reproductive cycles, rats were followed for 3–5 months, and all rats were euthanized at age 14–19 months.

Throughout the experiment, virgin rats were housed in standard conditions in groups of three rats per cage. Reproductive rats were housed in groups of three per cage during the pregnancy and post-weaning recovery periods, but were separated to one rat per cage during the last week of pregnancy and remained separated throughout lactation. Rats were fed a high-calcium diet (LabDiet 5001 Rodent Diet; 0.95% Ca). All experiments were performed in two batches, performed 11 months apart, with a final sample size of 4–5 reproductive rats and 6 virgin rats per batch. Experiments were performed unblinded.

2.2 μCT Scans

Starting at the first mating (week 0), the right proximal tibiae of all rats were scanned regularly at 10.5 μm voxel size using an *in vivo* μCT scanner (Scanco vivaCT40, Scanco Medical AG, Brüttisellen, Switzerland), with a radiation dosage of 0.639 Gy. During the first reproductive cycle (Cycle 1, weeks 0–12), rats were scanned weekly. Multiple studies have indicated that rats undergo minimal radiation damage during weekly scans (25,26). During the second and third cycles (Cycles 2 and 3, weeks 12–33), rats were scanned every three weeks, corresponding to the beginning of pregnancy, beginning of lactation, end of lactation, and middle and end of the post-weaning recovery. Virgin rats were scanned following the same schedule as the reproductive group. However, because the virgin rats underwent minimal changes in bone structure, fewer scans were analyzed during Cycle 1. For each *in vivo* scan, rats were anesthetized (4/2% isoflurane), and the right tibia was fixed using a custom holder (27). A 4.0 mm region of the proximal tibia located immediately below the growth plate was scanned at 10.5 μm resolution, with 200 ms integration time, 145 μA current, and 55 kVp energy, resulting in a total scan time of 20 minutes.

2.3 Image Registration

Sequential μCT scans obtained during the first reproductive cycle were registered to each other using a mutual-information-based, landmark-initialized, open-source registration toolkit (National Library of Medicine Insight Segmentation and Registration Toolkit) (28). The detailed methods have been published in our previous work (27,29). To track changes in trabecular bone microstructure during Cycle 1, a 2-mm-thick, trabecular VOI was identified in the week 12 scan (end of recovery after the first reproductive cycle) approximately 2.5 mm distal to the growth plate, and was then traced back to all the other Cycle 1 scans with the help of the transformation matrices based on the registrations. This procedure ensures that the same trabecular volume of interest (VOI) of each rat was longitudinally monitored during the first reproductive cycle. All VOIs were visually inspected to confirm accurate identification of the same trabecular region at all time points during Cycle 1.

Due to the unclosed growth plate in rodent long bone, the secondary spongiosa, where trabecular bone is commonly analyzed, undergoes longitudinal growth and endochondral ossification throughout an adult rat's life (24). Our previous study demonstrated a total of approximately 3.5 mm of bone growth in the proximal tibia from age 3 months to 20 months (24), making it impossible to trace the same VOI in the secondary spongiosa in rats over 3 reproductive cycles. However, between ages 4.5 and 7.5 months (approximate length of the first reproductive cycle), rats only underwent ~1 mm of longitudinal growth, demonstrating that it is possible to track the same trabecular VOI throughout a single reproductive cycle.

Therefore, analysis of trabecular microstructure within the first reproductive cycle was performed within a registered VOI, to allow precise tracking of changes in trabecular microarchitecture, whereas evaluation of trabecular structure over the course of three reproductive cycles was performed within an unregistered, 2-mm thick trabecular region located a constant 2.5mm distal to the proximal tibial growth plate to ensure consistency of evaluations throughout the study. In addition, we also performed a separate analysis to evaluate changes in trabecular microarchitecture over Cycles 2 and 3 within a registered VOI (please see Supplement).

2.4 Trabecular Microstructural Analysis

The μCT images within each VOI were Gaussian filtered (sigma=1.2, support=2) and thresholded using a global threshold (corresponding to 544 mg HA/cm^3), as determined through an adaptive thresholding algorithm provided by the scanner software. Trabecular bone structural parameters, including bone volume fraction (BV/TV), trabecular number (Tb.N), thickness (Tb.Th), and spacing (Tb.Sp), structure model index (SMI), and connectivity density (Conn.D) were measured for all rats (n=10 in reproductive group; n=12 in virgin group). For each rat, the percent change from baseline was computed for all trabecular parameters except SMI, which ranges between −3 to 3. Normalized SMI was computed by subtracting the baseline SMI from all follow-up measurements for each rat.

2.5 Trabecular Dynamics Analysis

μCT images taken during Cycle 1 at the beginning of pregnancy, at parturition, at weaning, and at 3 and 6 weeks of post-weaning recovery were used to assess the effects of reproduction on the structural deterioration and repair of individual trabeculae as well as rates of bone formation/resorption. Each scan was registered to the scan made 3 weeks previously, as described in 2.3. Following this registration, a 1.5×1.5×1 mm trabecular subvolume located 1.5 mm distal to the growth plate was extracted from the two images, which underwent a final registration to ensure an optimized alignment of trabecular features within the subvolume (30,31). To minimize interpolation bias induced by the image transformation, the follow-up and baseline images were both rotated through the same angle using our recently developed, matched-angle transformation scheme (31,32). The registered images were then filtered (Gaussian filter, sigma=1.2, support=2) and thresholded using a global threshold corresponding to 544 mg HA/cm^3.

The structural deterioration and repair of individual trabeculae occurring as a result of pregnancy, lactation, and post-weaning recovery were then measured in the precisely registered subvolumes through an individual trabecular dynamics (ITD) analysis, as described previously (30). Briefly, the trabecular rods and plates were isolated using individual trabecular segmentation (ITS) analysis (33), and the two registered subvolumes were compared to identify incidences of rod disconnection and plate perforation (measures of structural deterioration) and rod connection and plate perforation filling (measures of structural repair) (30).

Additionally, the bone formation and resorption rates were also measured based on the registered subvolumes. As described in (31), the registered, thresholded subvolumes were

subtracted from each other, and voxels of bone resorption were defined as voxels that were present in the scan made at the first time-point, but absent in scan made at the second time-point, whereas bone formation was defined as voxels that were absent in the initial scan, but were present at the second time-point. Based on the resulting, three-dimensional (3D) map of bone (re)modeling, bone formation and resorption rates were calculated as follows:

$$\text{Bone formation rate}={}^{\text{BFR}}\!/_{BS}=\frac{\text{volume of new bone formed}}{(\text{trabecular surface area})\cdot(\#\text{ days between scans})}$$

$$\text{Bone resorption rate}={}^{\text{BRR}}\!/_{BS}=\frac{\text{volume ofbone resorbed}}{(\text{trabecular surface area})\cdot(\#\text{days between scans})}$$

Please see Supplement for additional μCT-based measurements of trabecular bone dynamics.

These localized structural and (re)modeling evaluations necessitate extremely high image quality. The first batch of rats showed reduced image quality in the *in vivo* scan made at the end of lactation (week 6), due to the deterioration of the μCT scanner X-ray tube at this time point. Scans were thoroughly tested, and image quality was found to be sufficient to allow for accurate measures of standard, bulk trabecular bone quality (described in 2.4), however, the signal-to-noise ratio was not high enough to allow accurate evaluation of localized changes in trabecular microstructure/(re)modeling. Therefore, the *in vivo* dynamics analyses were performed only for the second batch of rats (5 reproductive and 6 virgins).

2.6 Cortical Bone Analysis

Cortical bone structure was analyzed in a 50-slice region of the proximal tibia located ~3.5 mm distal to the proximal growth plate over the course of 3 reproductive cycles for all rats (n=10 in reproductive group; n=12 in virgin group). During each cycle, measurements were made every 3 weeks: at the beginning of pregnancy, at parturition, at the end of lactation, and at 3 and 6 weeks post-weaning. Cortical bone was isolated using a semi-automated segmentation procedure similar to that described by Burghardt *et al.* (34), followed by application of a Gaussian filter (sigma=1.2, support=2) and global threshold corresponding to 709 mgHA/cm^3. Cortical bone parameters, including cortical area (Ct.Area), cortical thickness (Ct.Th), polar moment of inertia (pMOI), tissue mineral density (TMD), periosteal perimeter (P.Perim), and endosteal perimeter (E.Perim), were measured using the μCT scanner software (Scanco Medical). Cortical porosity was not evaluated, due to the inability to accurately measure porosity at the *in vivo* resolution of 10.5 μm.

2.7 Micro-Finite Element Analysis (μFEA)

Whole-bone stiffness was computed for a 1-mm thick region of the proximal tibia located 2.5 mm distal to the proximal growth plate for all rats (10 reproductive, 12 virgins) over the course of three reproductive cycles using a linear micro-finite element analysis (μFEA). Each μCT image was down-sampled by a factor of 1.5 (to a voxel size of 16 μm), the tibia was isolated from the fibula, and bone was segmented through application of a Gaussian filter (sigma=1.2, support=2), followed by a global threshold corresponding to 544 mg

HA/cm^3. Finite element models were constructed by converting each bone voxel to an eight-node brick element. Bone was then modeled as a linear elastic material with Young's modulus of 15 GPa and Poisson's ratio of 0.3 (35). An axial displacement of 0.01 mm was simulated, and the resulting reaction force was computed using a customized conjugate gradient solver, as described in (36). Whole-bone stiffness was calculated by dividing the reaction force by the displacement. Additionally, a load-share analysis was performed on μCT images taken at baseline and after 3 reproductive cycles in order to evaluate changes in the percentage of the load borne by the cortical and trabecular compartments. Briefly, the cortical bone at the proximal-most slice of the image stack undergoing μFEA, located 2.5 mm distal to the proximal growth plate, was isolated using a custom MATLAB script. The reaction forces exerted by the cortical and trabecular compartments at this slice after application of a simulated 0.01 mm compression of the 1-mm thick image stack were then computed. The cortical load-share fraction was defined as the fraction of the total force borne by the cortical compartment.

2.8 Tibia growth rate

During each scan, the total tibia length was estimated based on 2-D radiographs provided by the μCT scanner (scout view images). Total longitudinal growth was derived by computing changes in tibia length over time.

2.9 Statistics

All results are presented as mean ± standard deviation (SD). Changes in trabecular and cortical microstructural parameters as well as whole-bone stiffness over the course of each reproductive cycle in virgin and reproductive rats were evaluated by examining the interaction effects resulting from two-way, repeated-measures analysis of variance (ANOVA), corrected for baseline measures. Bonferroni corrections were applied to all *post hoc* tests. Comparisons between the two groups (virgin *vs.* reproductive) at baseline as well as at the end of each reproductive cycle were made using Student's T-tests. Due to differences in the time points assessed between reproductive and virgin rats, changes over time for the registered comparisons within Cycle 1 were evaluated separately for the reproductive group using a repeated-measures, one-way ANOVA.

Differences in bone formation/resorption and structural deterioration/repair during pregnancy, lactation, post-weaning, and in virgin rats were evaluated using one-way ANOVA, with Bonferroni *post hoc* corrections. Finally, comparisons of the cortical loadshare fraction in virgin *vs.* reproductive rats before and after 3 reproductive cycles were made using a 2-way, repeated-measures ANOVA, covaried by baseline values, with Bonferroni *post hoc* corrections.

P-values less than 0.05 were considered significant, while p-values below 0.1 are reported as a trend of difference with the specific p-value provided.

3. Results

3.1 Changes in trabecular microstructure during the first reproductive cycle

At baseline (age 4–5 months) rats weighed 293 ± 23 g and had trabecular BV/TV, Tb.Th, Tb.N, Tb.Sp, SMI, and Conn.D of 0.34, 0.081 mm, 5.51 mm^{-1}, 0.164 mm, 1.03, and 154 mm^{-3}, respectively at the proximal tibia. There were no differences in baseline measures of trabecular microarchitecture between the reproductive and virgin groups. Virgin rats underwent no changes in any trabecular parameters during the experiment (Figure 1). On the other hand, in the reproductive rats, all parameters measured underwent dramatic changes over the course of Cycle 1 (Figure 1). BV/TV, Tb.Th, Tb.N, SMI, and Conn.D did not change during the first two weeks of pregnancy, but began to change rapidly during the third week of pregnancy (third trimester). At parturition, BV/TV, Tb.Th, Tb.N, and Conn.D were 42%, 12%, 21% and 51% lower than at baseline, respectively. SMI was significantly elevated relative to baseline. Trabecular microarchitecture continued to decline steadily throughout the lactation period, and at the end of lactation, BV/TV, Tb.Th, Tb.N, and Conn.D were 85%, 33%, 59%, and 90% below their baseline values, while Tb.Sp had increased to 227% above baseline and SMI was 1.86 above baseline.

The extent of recovery following weaning was highly variable for the different trabecular parameters. BV/TV increased gradually after weaning, and 6 weeks after weaning, BV/TV was 131% greater than at the end of lactation. However, at the end of the recovery period, the BV/TV remained 67% lower than it was at baseline, and at the end of the first reproductive cycle, BV/TV of the reproductive rats was 64% lower than that of virgin rats at the same time point. In contrast to BV/TV, Tb.N, Tb.Sp, SMI, and Conn.D did not recover after weaning, as at 6 weeks post-weaning, none of these parameters were significantly different from the end of lactation. At the end of recovery, Tb.Sp remained 190% above baseline and SMI remained elevated over baseline by 1.42, while Tb.N and Conn.D remained 56% and 83% below baseline, respectively. Finally, in contrast to all other measures, Tb.Th recovered fully during the 6-week post-weaning period, as at the end of recovery, Tb.Th was not different from baseline and was not different between reproductive and age-matched virgin rats.

3.2 Effects of reproduction on trabecular dynamics during the first reproductive cycle

During pregnancy, BRR/BS was significantly elevated in the reproductive rats (406% greater than virgins; Figure 2B). BRR/BS further increased to 737% greater than virgin rats during the lactation period. Meanwhile, during both pregnancy and lactation, BFR/BS remained similar to virgin rats. After weaning, BRR/BS in the reproductive rats dropped by 89% to similar levels as virgin rats, and remained low. In contrast, during the first three weeks of the post-weaning recovery, BFR/BS increased to 1016% greater than virgins (Figure 2C). BFR/BS then declined significantly by 67% during the second recovery phase, correlating with the plateau in BV/TV that was observed after the first three weeks of recovery.

ITD-based measurements of structural deterioration and repair followed similar trends to *in vivo* dynamic bone histomorphometry measurements (Figure 2 D,E). Reproductive rats had a 266% and 194% elevated rate of structural deterioration (measured as the number of

incidences of trabecular plate perforation and rod disconnection per mm^3) during pregnancy and lactation, respectively, as compared to virgins. This elevation in structural deterioration rate was largely due to increases in rod disconnection, as rod disconnections constituted an average of 83% of instances of structural deterioration during the pregnancy and lactation periods. After weaning, the rate of structural deterioration decreased by 93%, and remained low throughout the post-weaning recovery period. Reproductive rats showed low rates of structural repair (defined as the number of incidences of plate perforation filling and rod connection per mm^3) during both pregnancy and lactation, similar to virgin rats. Rates of structural repair were then elevated over the first half of post-weaning recovery (1475% greater than during lactation). A majority of 86% of the instances of structural repair during the first three weeks post-weaning occurred as a result of rod connection, whereas plate perforation filling constituted on average 14% of instances of structural repair. The rate of structural repair then declined back to baseline levels during the second half of the post-weaning period.

3.3 Cumulative changes in trabecular microstructure over three repeated reproductive cycles

Evaluation of trabecular microstructure over the course of three consecutive cycles of pregnancy, lactation, and post-weaning recovery indicates significant variations in the extent of trabecular deterioration over the different reproductive cycles (Figure 3). As described in 3.1, during the pregnancy of the first reproductive cycle, BV/TV, SMI, and Conn.D all underwent a dramatic deterioration. On the other hand, reproductive rats underwent no significant changes in any trabecular parameters during the pregnancy phase of the second and third cycles.

In addition to variations in the extent of pregnancy-induced bone loss, the amount of bone loss taking place during lactation also varied depending on the reproductive cycle. Reproductive rats underwent 39–73% declines in BV/TV and 17–22% reductions in Tb.Th during the lactation phase of all three reproductive cycles. However, while the SMI increased by 0.58 and Conn.D decreased by 79% during lactation of the first reproductive cycle, neither parameter underwent significant changes during the lactation phase of subsequent cycles. Additionally, Tb.N underwent a dramatic, 49% reduction and Tb.Sp underwent a substantial 125% increase during the first lactation, but neither parameter underwent significant changes during the lactation phase of the second reproductive cycle, and Tb.N decreased by only 19% while Tb.Sp increased by only 22%, during the third lactation.

Post-weaning recovery appeared to be fairly consistent among the different reproductive cycles. Parameters that underwent minimal recovery (Tb.N, Tb.Sp, SMI, and Conn.D) during the first reproductive cycle also did not show substantial improvement during the post-weaning phase of subsequent cycles. BV/TV, which recovered partially after weaning during the first reproductive cycle, also showed a partial post-weaning recovery after Cycles 2 and 3. Although there was no significant increase between BV/TV at the end of the second lactation and BV/TV at the end of the second weaning phase (weeks 18 and 21), the BV/TV at the end of the second weaning phase (week 21) was no longer significantly different from that at the beginning of the second cycle (week 12), indicating at least a partial recovery

during this cycle. Finally, Tb.Th, which showed a full recovery at the end of the first reproductive cycle, also underwent a complete recovery following Cycle 2, and, after Cycle 3, the Tb.Th even recovered to values 10% higher than those found prior to the third pregnancy. Over the same time period corresponding to the three reproductive cycles, virgin rats showed no significant changes in any trabecular parameters.

Cumulatively, three reproductive cycles resulted in dramatic alterations of trabecular microarchitecture: While there were no significant differences between reproductive and virgin rats in any of the parameters at baseline, after three reproductive cycles, reproductive rats showed a trabecular microstructure which had 59% lower BV/TV, 55% lower Tb.N, 166% greater Tb.Sp, 0.74 greater SMI, and 82% lower Conn.D, but 20% greater Tb.Th than that of virgin rats at the same time point. Thus, reproduction induced deteriorations in the trabecular microstructure, but increased the average thickness of the remaining trabeculae, as compared to virgins (Figure 3).

3.4 Effects of reproduction on cortical bone structure

Reproduction also resulted in substantial changes in cortical bone structure at the proximal tibia, in particular during the first reproductive cycle (Figure 4). Specifically, the pMOI, Ct.Area, and Ct.Th increased 10%, 9%, and 12%, respectively, in reproductive rats during the first pregnancy. pMOI, Ct.Area, and Ct.Th then decreased 17%, 16%, and 14%, during the lactation phase of the first reproductive cycle. Over the 6-week post-weaning period, pMOI, Ct.Area, and Ct.Th increased 9%, 14% and 17%, respectively,, and at the end of the first reproductive cycle, reproductive rats showed no remaining differences from baseline in pMOI or Ct.Area, and showed a slight, 13% elevated Ct.Th. Subsequent reproductive cycles resulted in reduced magnitude changes in cortical bone structure, with pMOI undergoing 10% and 7% increases during the second and third pregnancies, respectively, with no significant changes during the second and third lactation phases. Ct. Area increased 6% during both the second and third pregnancies followed by 4–5% decreases during the second and third lactation periods (as compared to a 9% increase during the first pregnancy and 16% reduction during the first lactation). Similarly, Ct.Th showed modest 5% increases during the second and third pregnancies, and underwent slight 4–6% decreases during the second and third lactation periods. Apart from an 11% thickening of the cortical bone over weeks 0–12, and a 4% increase in pMOI over weeks 21–33, virgin rats showed no significant changes in pMOI, Ct.Area, or Ct.Th over the course of the study.

In contrast, the TMD of both reproductive and virgin rats increased consistently, in particular during the first reproductive cycle, and at the end of Cycle 1, TMD was 7% greater than baseline in both virgin and reproductive rats. Both groups of rats underwent minimal changes in P.Perim and E.Perim throughout the experiment, with virgins undergoing no changes in either parameter, while the reproductive group showed a slight, 2% increase in P.Perim during the second reproductive cycle, and a 2% decrease in E.Perim during the third cycle.

All together, although there were no differences between reproductive and virgin rats in pMOI, Ct.Area, Ct.Th, or TMD at baseline, the three repeated reproductive cycles resulted in substantial differences between virgin and reproductive rats at the end of the experiment.

After three cycles, reproductive rats showed a 13% greater pMOI, 9% greater Ct.Area, 1% reduced TMD, and a trend towards a 7% greater Ct.Th relative to virgins. Reproductive rats showed a consistently 4% elevated P.Perim as compared to virgin rats throughout the experiment, and although reproductive rats showed a trend towards a 6% greater E.Perim at baseline, there was no longer any difference in E.Perim between the two groups of rats after 3 reproductive cycles. Taken together, these results indicate that, after three reproductive cycles, the cortical bone at the proximal tibia had slightly lower mineralization, but increased robustness (in the form of elevated pMOI, Ct.Area, and Ct.Th), in reproductive rats as compared to virgins.

3.5 Reproduction-induced changes in tibia mechanical properties

μFEA-derived measures of whole-bone stiffness changed most dramatically during the first reproductive cycle (Figure 5A), where reproductive rats showed a 34% decrease in whole-bone stiffness during lactation. This recovered partially after weaning, as the whole-bone stiffness increased 39% over the 6-week post-weaning period. During the second and third reproductive cycles, reproductive rats showed 18% and 14% decreases in stiffness as a result of lactation, with 11% and 18% increases in stiffness over the second and third post-weaning periods In contrast, virgin rats showed no changes in whole-bone stiffness throughout the experiment. Reproductive-associated changes in stiffness appeared to recover fully over the course of three reproductive cycles, as there was no difference in whole-bone stiffness between reproductive and virgin rats at the end of the experiment.

The cortical load-share fraction, or the percentage of the total load carried by the cortical bone (Figure 5B) was computed both before and after the three repeated reproductive cycles. As shown in Figure 5C, at baseline, there was no difference in cortical load-share fraction between reproductive and virgin rats, indicating that in both groups, the cortical bone carried 68% of the total load applied to the tibia. Virgin rats showed no substantial change in cortical load-share fraction over the course of the experiment. However, in reproductive rats, the cortical load-share fraction was significantly elevated to 87% at the end of the experiment.

3.6 Effects of reproduction on longitudinal tibia growth

Comparison of the changes in total tibia length in reproductive and virgin rats over the course of the first, second, and third reproductive cycles indicated a significant, 2–3% increase in tibia length during Cycle 1 in both groups ($p<0.05$; Figure 4G). Virgin rats showed no significant changes in tibia length over the course of Cycles 2 or 3, indicating that these rats underwent minimal longitudinal growth over these time periods. In contrast, while reproductive rats also showed no significant changes in tibia length during Cycle 2, this group did show a significant, 1.9% increase in tibia length during Cycle 3 ($p<0.05$), indicating an elevated growth rate during this cycle in reproductive rats as compared to virgins. Group-wise comparisons at the end of each cycle indicated that, by the end of Cycles 2 and 3, reproductive rats had undergone significantly greater increases in tibia length than virgins ($p<0.05$), resulting in a 2.3% and 4.6% greater total tibia length in reproductive rats than in virgins at the end of the second and third reproductive cycles, respectively ($p<0.05$).

4. Discussion

This study forms the first *in vivo*, longitudinal tracking of the changes taking place as a result of pregnancy, lactation, and post-weaning recovery at the proximal tibia in rats. Based on previous rodent studies, combined with results from clinical studies indicating that reproductive bone loss has no long-term adverse effect on maternal bone health (15–21), we hypothesized that reproduction would induce a substantial bone loss, which would recover following weaning. Therefore, the initial aim of this study was to investigate the structural mechanisms behind reproductive bone loss and recovery of the trabecular bone at the proximal tibia. Our longitudinal approach allowed for the tracking of local changes in the trabecular bone within a constant volume of interest (VOI) over the course of a complete cycle of pregnancy, lactation, and post-weaning recovery. Trabeculae underwent thinning as well as dramatic structural deterioration during the last week of pregnancy as well as throughout the lactation period. This result is consistent with what has been found in previous rodent evaluations of skeletal changes during lactation (6–8,37–40). Additionally, the elevated bone resorption rates during the lactation phase measured through μCT-based trabecular dynamics analysis agree with results previously reported by Miller and Bowman (10), who demonstrated that a dramatically elevated fraction of the tibial trabecular bone surface was covered by osteoclasts during lactation (10). Previous studies investigating the effects of pregnancy on trabecular bone have been less clear, with some studies finding minimal effects of pregnancy on the quantity of trabecular bone (7,39), while others found evidence of increased bone resorption over this time period (41). Similarly, clinical studies have found controversial results regarding the effects of pregnancy on maternal bone in humans (3). Discrepancies regarding the effect of pregnancy may be due in part to differences in the stage of pregnancy investigated among the different studies, as our findings indicate substantial bone loss taking place only during the last week (equivalent to the third trimester) before parturition.

Following weaning, we found an initial increase in the rate of bone formation and structural recovery, leading to a small increase in BV/TV. This partial recovery of trabecular bone volume appeared to occur through a thickening of the remaining trabeculae, with minimal recovery in trabecular microarchitecture, as the Tb.Th recovered fully following weaning, while minimal changes were seen in Tb.N, Conn.D, or SMI. Additionally, as indicated by ITD analysis, the extent of structural repair taking place post-weaning was substantially lower than the amount of pregnancy- and lactation-induced structural deterioration, further suggesting an incomplete recovery of trabecular microarchitecture. Previous studies have found variable results regarding the extent of recovery post-weaning. Consistent with our *in vivo* dynamic bone histomorphometry results, the maternal skeleton has been shown to undergo an anabolic phase shortly after weaning, with a reduction in bone resorption activities and an elevated rate of bone formation (9–12,40). In particular, fluorescent-labeled histomorphometry studies indicate a ~600% increase in BFR/BS at the proximal tibia post-weaning (11), similar to the ~1000% increase in 3D BFR/BS found in our *in vivo* dynamic bone histomorphometry measurements. Additionally, previous studies evaluating bone density and microstructure indicate a greater bone volume and improved quality after post-weaning recovery compared to at the end of lactation (6,9,11,13,40,42,43). Furthermore,

multiple clinical studies indicate no adverse effects of reproductive or lactation history on post-menopausal fracture risk (15–21), indicating that reproductive bone loss constitutes a transient process which does not adversely affect bone health in the long-term (2,15–21).On the other hand, similar to our findings, multiple rodent (6,9,11,13,42,43) and clinical (44,45) studies have indicated that even after a post-weaning recovery period, the maternal bone continues to show some remaining structural and/or mechanical deficits relative to controls. Taken together, these contradictory findings that despite a period of post-weaning recovery, reproduction induces permanent alterations in trabecular microstructure, without adversely affecting long-term bone health, would suggest that there may be an alternate mechanism to compensate for the observed low rates of trabecular bone recovery post-weaning.

Thus, we next investigated the effect of multiple reproductive cycles on the tibial trabecular as well as cortical bone. In contrast to the first cycle, subsequent reproductive cycles revealed minimal changes in trabecular bone microstructure during the pregnancy phase. On the other hand, lactation-induced deterioration of trabecular microstructure and thickness, and post-weaning recovery of trabecular thickness, followed similar trends over the course of all three cycles, although trabecular microarchitectural changes were more dramatic during the first reproductive cycle than the second and third. Additionally, reproduction-induced changes in cortical bone were larger during the first cycle of pregnancy and lactation, as pMOI, Ct.Area, and Ct.Th underwent substantial changes during the first reproductive cycle, but changed much less dramatically as a result of subsequent cycles. Changes in cortical bone during the first reproductive cycle were similar to those found by Miller *et al.* (39) and Vajda *et al.* (40), who also found an increased Ct.Area in rats at the end of pregnancy, and a reduced Ct.Area at the end of lactation, relative to controls. Furthermore, previous studies of reproductive metabolism have indicated that later cycles of pregnancy and lactation are more efficient than the first (43,46), which may help to explain our findings of greater trabecular and cortical bone loss over the first cycle of pregnancy and lactation, as compared to subsequent cycles.

Overall, the cumulative effect of three repeated cycles of pregnancy, lactation, and weaning resulted in a substantially altered trabecular as well as cortical architecture. After three reproductive cycles, the trabecular network of reproductive rats was characterized by fewer, less connected, and more rod-like, but also, on average, thicker trabecular elements than that of virgin controls. This finding of a substantially altered trabecular microstructure after multiple reproductive cycles is in agreement with a cross-sectional study by Bowman *et al.*, who also found that, after 6 weeks of recovery from two successive reproductive cycles, rats continued to show substantially reduced trabecular BV/TV at the tibial metaphysis relative to nulliparous controls (11). Interestingly, after 3 reproductive cycles, the cortical bone of reproductive rats appeared to be more robust, with a greater pMOI, Ct.Area, and Ct.Th in reproductive rats than controls. This is consistent with a clinical study indicating that women who underwent a long duration of breastfeeding (more than 33 months) had a greater tibial cross-sectional moment of inertia compared with women who breastfed for less than 12 months when assessed ~16 years after the last lactation (23). Additionally, FEA-derived measurements of whole-bone stiffness showed no difference between reproductive and virgin rats at the end of three reproductive cycles, indicating that, although reproduction induced transient changes in whole-bone stiffness,, there did not appear to be any significant

long-term effect of reproduction on the mechanical integrity of the bone in spite of the substantially altered trabecular and cortical microarchitecture. This result is consistent with previous mechanical testing-based studies carried out in rats, as Vajda *et al.* found a decrease in vertebral and femoral stiffness in reproductive rats as a result of lactation, with no remaining significant difference in stiffness between reproductive rats and nulliparous controls at 8 weeks post-weaning (40).

The lack of difference between reproductive and virgin rats in whole-bone stiffness at week 33, combined with the apparently irreversible trabecular deterioration and the increased robustness of post-reproductive cortical bone, suggest that the cortical bone may be able to compensate for trabecular bone deficits, allowing the bone to maintain its mechanical integrity after reproduction in spite of the incomplete recovery of the trabecular microarchitecture. In particular, reproduction may induce a redistribution of load between the cortical and trabecular compartments, where the cortical bone of post-reproductive rats may carry a larger proportion of the load applied to the bone. The last portion of our study sought to investigate this question by evaluating the fraction of the total load carried by the cortical and trabecular compartments in virgin and reproductive rats. Indeed, we found that in reproductive rats, the percentage of the total load borne by the cortical bone increased significantly after three reproductive cycles, while no changes were found in the cortical loadshare fraction of virgin rats over the same time period. This leads us to conclude that reproduction may lead to a redistribution of mechanical functions, where cortical bone carries a larger proportion of the load in post-reproductive bone, which, in turn, could help to explain the paradox that reproduction leads to bone loss with incomplete recovery without increasing postmenopausal risk of osteoporosis or fracture.

Estimation of longitudinal bone growth at the proximal tibia also suggested a significant effect of reproduction on whole-bone growth rate, as reproductive rats were found to undergo greater increases in tibia length than virgins over the course of multiple reproductive cycles. Previous cross-sectional studies evaluating the effects of reproduction on long-bone growth based on fluorescent markers identified on histological sections, have indicated elevated growth in rats during pregnancy, which slowed during lactation, and then resumed during the post-weaning period (43,47). Thus, we expect that our observed differences in total tibial growth between reproductive and virgin rats over the course of a complete reproductive cycle are a result of the cumulative effects of altered growth rates during pregnancy, lactation, and post-weaning. However, our method of evaluating tibial growth based on 2-D radiographs was limited in its temporal resolution and thus, although we were able to quantify altered tibial growth over the course of a complete reproductive cycle, this method lacked the precision to detect changes in tibial growth rate during the individual phases of pregnancy, lactation, and weaning within each cycle. Thus further longitudinal studies are required to clarify the precise effects of each reproductive phase on tibial growth.

Our finding that reproductive rats exhibit elevated longitudinal bone growth also suggests a modeling-based component to the effects of reproduction on trabecular and cortical bone microstructure, through changes in endochondral ossification from the growth plate. For instance, it is possible that, in addition to increases in bone formation on the surfaces of

existing trabeculae, the development of new trabecular elements from the growth plate through endochondral ossification may also play a small role in the increase in trabecular bone mass observed post-weaning. Altered patterns of endochondral ossification may also play a part in inducing the changes in cortical bone structure observed during reproduction, as the elevated cortical pMOI and Ct.Area observed in reproductive rats compared to virgins after 3 reproductive cycles may partially be a result of their altered longitudinal growth. However, further studies are required to clarify the relationship between the reproduction-based changes in longitudinal bone growth and the effects on metaphyseal cortical and trabecular microstructure.

This study is novel in its longitudinal design, allowing precise, long-term tracking of reproduction-induced changes in maternal rat bone. However, there are inherent limitations to this design: Notably, this study utilizes a rat model. Although rat bone has been shown to be highly representative of the changes undergone by human bone under similar conditions, the precise implications of the findings of this study for human health remain to be confirmed in a clinical study. Notably, the reduced extent of bone loss experienced by women as compared to rodents as a result of reproduction and lactation may induce altered patterns of trabecular and cortical bone loss and compensation in humans than those reported here for rats. However, a preliminary longitudinal study using high-resolution peripheral quantitative CT (HR-pQCT) to evaluate microstructural changes in women in response to lactation indicated a significant, 3% reduction in inner trabecular density at the distal radius over the course of 6 months of lactation, which persisted 6 months post-weaning (48), consistent with our findings of persistent reproductive trabecular bone loss in rats. Similarly, a more recent HR-pQCT based study also showed 2.6% reduced trabecular thickness and 2.6% reduced BV/TV at the distal tibia at 12-months post-partum in women who had lactated for at least 9 months (49) The increasing availability of HR-pQCT scanners means that a complete, longitudinal, clinical investigation of the long-term impact of pregnancy, lactation and weaning on bone microstructure will be possible in the near future.

Additionally, our study evaluates reproductive changes at a single skeletal site. The proximal tibia is a commonly investigated site in preclinical studies of osteoporosis pathophysiology and treatment, and changes at the proximal tibia have been shown to be highly relevant to human health. However, location-specific effects must be considered when applying the results of this study to different skeletal sites. We are currently conducting an on-going study to examine effects of reproduction on multiple skeletal sites in rats. Our study is also limited by the baseline differences in E.Perim and P.Perim found between the reproductive and virgin groups. Although rats were randomly assigned to the two groups at the start of the experiment, we did find a greater P.Perim and a trend towards a greater E.Perim in the reproductive group as compared to the virgins at week 0 (in spite of finding no significant baseline differences between the two groups in any of the other parameters). Thus, this baseline difference in cortical bone structure needs to be considered when interpreting the results of our cortical analysis. Finally, our study is limited by the available spatial resolution of *in vivo* μCT images. Although the 10.5 μm voxel size was sufficient for all the measurements reported here, an *in vivo* measurement of reproduction-induced changes in cortical bone porosity was not possible at this resolution.

In spite of its limitations, this study provides a thorough, longitudinal evaluation of the effects of pregnancy, lactation, and weaning on maternal bone, allowing important insight into the processes taking place during and after reproduction. Taken together, our results indicate that pregnancy and lactation result in both long-term and short-term alterations in trabecular microstructure, with the trabecular thickness undergoing a transient reduction which is fully recovered after weaning, while the trabecular microarchitecture undergoes a substantial deterioration, which recovers minimally. In contrast to trabecular bone structure, our study shows an improved robustness of cortical bone, as well as an increase in the proportion of the total load carried by the cortical bone as a result of reproduction. This may compensate for the irreversible trabecular deterioration taking place, resulting in no long-term effect of reproduction on whole-bone stiffness at the proximal tibia.

Supplementary Material

Refer to Web version on PubMed Central for supplementary material.

Acknowledgments

Research reported in this publication was supported by the Penn Center for Musculoskeletal Diseases (PCMD) NIH/NIAMSP30AR050950, NIH/NIAMS R03-AR065145 (to XSL), National Science Foundation Graduate Research Fellowship (to CMJdB), and NIH/NIAMS T32-AR007132 (to CMJdB).

Authors' roles:

Study design: XSL, CMJdB, ARAS. Study conduct: CMJdB, ARAS, WJT. Data collection: CMJdB, YL, CL, ARAS, WJT. Data analysis: CMJdB, ARAS, YL, CL. Data interpretation: XSL, CMJdB. Drafting manuscript: CMJdB. Revising manuscript content: XSL, ARAS, YL, WJT, CL. Approving final version of manuscript: XSL, CMJdB, ARAS, YL, WJT, CL. XSL and CMJdB take responsibility for the integrity of the data analysis.

References

1. Kovacs CS. Calcium and bone metabolism disorders during pregnancy and lactation. Endocrinol Metab Clin North Am. 2011; 40(4):795–826. [PubMed: 22108281]
2. Kovacs CS, Ralston SH. Presentation and management of osteoporosis presenting in association with pregnancy or lactation. Osteoporos Int. 2015
3. Ensom MH, Liu PY, Stephenson MD. Effect of pregnancy on bone mineral density in healthy women. Obstet Gynecol Surv. 2002; 57(2):99–111. [PubMed: 11832786]
4. Sowers M, Corton G, Shapiro B, et al. Changes in bone density with lactation. JAMA. 1993; 269(24):3130–5.
5. Kent GN, Price RI, Gutteridge DH, et al. Human lactation: forearm trabecular bone loss, increased bone turnover, and renal conservation of calcium and inorganic phosphate with recovery of bone mass following weaning. J Bone Miner Res. 1990; 5(4):361–9. [PubMed: 2343775]
6. Liu XS, Ardeshirpour L, VanHouten JN, Shane E, Wysolmerski JJ. Site-specific changes in bone microarchitecture, mineralization, and stiffness during lactation and after weaning in mice. J Bone Miner Res. 2012; 27(4):865–75. [PubMed: 22189918]
7. VanHouten JN, Wysolmerski JJ. Low estrogen and high parathyroid hormone-related peptide levels contribute to accelerated bone resorption and bone loss in lactating mice. Endocrinology. 2003; 144(12):5521–9. [PubMed: 14500568]
8. Zeni SN, Di Gregorio S, Mautalen C. Bone mass changes during pregnancy and lactation in the rat. Bone. 1999; 25(6):681–5. [PubMed: 10593413]
9. Ardeshirpour L, Dann P, Adams DJ, et al. Weaning triggers a decrease in receptor activator of nuclear factor-kappaB ligand expression, widespread osteoclast apoptosis, and rapid recovery of bone mass after lactation in mice. Endocrinology. 2007; 148(8):3875–86. [PubMed: 17495007]

10. Miller SC, Bowman BM. Rapid inactivation and apoptosis of osteoclasts in the maternal skeleton during the bone remodeling reversal at the end of lactation. Anat Rec (Hoboken). 2007; 290(1):65–73. [PubMed: 17441199]
11. Bowman BM, Siska CC, Miller SC. Greatly increased cancellous bone formation with rapid improvements in bone structure in the rat maternal skeleton after lactation. J Bone Miner Res. 2002; 17(11):1954–60. [PubMed: 12412802]
12. Miller SC, Anderson BL, Bowman BM. Weaning initiates a rapid and powerful anabolic phase in the rat maternal skeleton. Biol Reprod. 2005; 73(1):156–62. [PubMed: 15788754]
13. Miller SC, Bowman BM. Rapid improvements in cortical bone dynamics and structure after lactation in established breeder rats. Anat Rec A Discov Mol Cell Evol Biol. 2004; 276(2):143–9. [PubMed: 14752853]
14. Qing H, Ardeshirpour L, Pajevic PD, et al. Demonstration of osteocytic perilacunar/canalicular remodeling in mice during lactation. J Bone Miner Res. 2012; 27(5):1018–29. [PubMed: 22308018]
15. Cummings SR, Nevitt MC, Browner WS, et al. Risk factors for hip fracture in white women. Study of Osteoporotic Fractures Research Group. N Engl J Med. 1995; 332(12):767–73. [PubMed: 7862179]
16. Cure-Cure C, Cure-Ramirez P, Teran E, Lopez-Jaramillo P. Bone-mass peak in multiparity and reduced risk of bone-fractures in menopause. Int J Gynaecol Obstet. 2002; 76(3):285–91. [PubMed: 11880132]
17. Hillier TA, Rizzo JH, Pedula KL, et al. Nulliparity and fracture risk in older women: the study of osteoporotic fractures. J Bone Miner Res. 2003; 18(5):893–9. [PubMed: 12733729]
18. Kauppi M, Heliovaara M, Impivaara O, Knekt P, Jula A. Parity and risk of hip fracture in postmenopausal women. Osteoporos Int. 2011; 22(6):1765–71. [PubMed: 20924749]
19. Mori T, Ishii S, Greendale GA, et al. Parity, lactation, bone strength, and 16-year fracture risk in adult women: findings from the Study of Women's Health Across the Nation (SWAN). Bone. 2015; 73:160–6. [PubMed: 25528102]
20. Petersen HC, Jeune B, Vaupel JW, Christensen K. Reproduction life history and hip fractures. Ann Epidemiol. 2002; 12(4):257–63. [PubMed: 11988414]
21. Taylor BC, Schreiner PJ, Stone KL, et al. Long-term prediction of incident hip fracture risk in elderly white women: study of osteoporotic fractures. J Am Geriatr Soc. 2004; 52(9):1479–86. [PubMed: 15341549]
22. Streeten EA, Ryan KA, McBride DJ, et al. The relationship between parity and bone mineral density in women characterized by a homogeneous lifestyle and high parity. J Clin Endocrinol Metab. 2005; 90(8):4536–41. [PubMed: 15899951]
23. Wiklund PK, Xu L, Wang Q, et al. Lactation is associated with greater maternal bone size and bone strength later in life. Osteoporos Int. 2012; 23(7):1939–45. [PubMed: 21927916]
24. Altman AR, Tseng WJ, de Bakker CM, et al. Quantification of skeletal growth, modeling, and remodeling by in vivo micro computed tomography. Bone. 2015; 81:370–9. [PubMed: 26254742]
25. Brouwers JE, van Rietbergen B, Huiskes R. No effects of in vivo micro-CT radiation on structural parameters and bone marrow cells in proximal tibia of wistar rats detected after eight weekly scans. J Orthop Res. 2007; 25(10):1325–32. [PubMed: 17568420]
26. Klinck RJ, Campbell GM, Boyd SK. Radiation effects on bone architecture in mice and rats resulting from in vivo micro-computed tomography scanning. Med Eng Phys. 2008; 30(7):888–95. [PubMed: 18249025]
27. Lan S, Luo S, Huh BK, et al. 3D image registration is critical to ensure accurate detection of longitudinal changes in trabecular bone density, microstructure, and stiffness measurements in rat tibiae by in vivo microcomputed tomography (muCT). Bone. 2013; 56(1):83–90. [PubMed: 23727434]
28. Johnson HJ, McCormick M, Ibanez L, Consortium IS. The ITK Software Guide. 2013
29. Altman AR, Tseng WJ, de Bakker CM, et al. A closer look at the immediate trabecula response to combined parathyroid hormone and alendronate treatment. Bone. 2014; 61C:149–157.

30. Altman AR, De Bakker CM, Tseng WJ, et al. Enhanced individual trabecular repair and its mechanical implications in parathyroid hormone and alendronate treated rat tibial bone. Journal of Biomechanical Engineering. 2015; 137(1):011004–7.
31. de Bakker CM, Altman AR, Tseng WJ, et al. muCT-based, in vivo dynamic bone histomorphometry allows 3D evaluation of the early responses of bone resorption and formation to PTH and alendronate combination therapy. Bone. 2015; 73C:198–207.
32. de Bakker CM, Altman AR, Li C, et al. Minimizing Interpolation Bias and Precision Error in In Vivo microCT-Based Measurements of Bone Structure and Dynamics. Ann Biomed Eng. 2016; 44(8):2518–28. [PubMed: 26786342]
33. Liu XS, Sajda P, Saha PK, et al. Complete volumetric decomposition of individual trabecular plates and rods and its morphological correlations with anisotropic elastic moduli in human trabecular bone. J Bone Miner Res. 2008; 23(2):223–35. [PubMed: 17907921]
34. Burghardt AJ, Buie HR, Laib A, Majumdar S, Boyd SK. Reproducibility of direct quantitative measures of cortical bone microarchitecture of the distal radius and tibia by HR-pQCT. Bone. 2010; 47(3):519–28. [PubMed: 20561906]
35. Guo XE, Goldstein SA. Is trabecular bone tissue different from cortical bone tissue? Forma. 1997; 12:185–196.
36. Hollister SJ, Brennan JM, Kikuchi N. A homogenization sampling procedure for calculating trabecular bone effective stiffness and tissue level stress. J Biomech. 1994; 27(4):433–44. [PubMed: 8188724]
37. Ardeshirpour L, Brian S, Dann P, VanHouten J, Wysolmerski J. Increased PTHrP and decreased estrogens alter bone turnover but do not reproduce the full effects of lactation on the skeleton. Endocrinology. 2010; 151(12):5591–601. [PubMed: 21047946]
38. Miller SC, Bowman BM. Comparison of bone loss during normal lactation with estrogen deficiency osteopenia and immobilization osteopenia in the rat. Anat Rec. 1998; 251(2):265–74. [PubMed: 9624458]
39. Miller SC, Shupe JG, Redd EH, Miller MA, Omura TH. Changes in bone mineral and bone formation rates during pregnancy and lactation in rats. Bone. 1986; 7(4):283–7. [PubMed: 3768208]
40. Vajda EG, Bowman BM, Miller SC. Cancellous and cortical bone mechanical properties and tissue dynamics during pregnancy, lactation, and postlactation in the rat. Biol Reprod. 2001; 65(3):689–95. [PubMed: 11514329]
41. Marie PJ, Cancela L, Le Boulch N, Miravet L. Bone changes due to pregnancy and lactation: influence of vitamin D status. Am J Physiol. 1986; 251(4 Pt 1):E400–6. [PubMed: 3766725]
42. Bornstein S, Brown SA, Le PT, et al. FGF-21 and skeletal remodeling during and after lactation in C57BL/6J mice. Endocrinology. 2014; 155(9):3516–26. [PubMed: 24914939]
43. Bowman BM, Miller SC. Skeletal mass, chemistry, and growth during and after multiple reproductive cycles in the rat. Bone. 1999; 25(5):553–9. [PubMed: 10574575]
44. Affinito P, Tommaselli GA, di Carlo C, Guida F, Nappi C. Changes in bone mineral density and calcium metabolism in breastfeeding women: a one year follow-up study. J Clin Endocrinol Metab. 1996; 81(6):2314–8. [PubMed: 8964870]
45. More C, Bettembuk P, Bhattoa HP, Balogh A. The effects of pregnancy and lactation on bone mineral density. Osteoporos Int. 2001; 12(9):732–7. [PubMed: 11605738]
46. Kunkele J, Kenagy GJ. Inefficiency of lactation in primiparous rats: the costs of first reproduction. Physiol Zool. 1997; 70(5):571–7. [PubMed: 9279924]
47. Redd EH, Miller SC, Jee WS. Changes in endochondral bone elongation rates during pregnancy and lactation in rats. Calcif Tissue Int. 1984; 36(6):697–701. [PubMed: 6442205]
48. Kokolus S, Vrabel MB, Liu XS, et al. High resolution peripheral quantitative CT (HRpQCT) reveals preferential inner trabecular bone loss in lactating women American Society for Bone and Mineral Research 32nd Annual Meeting. 2010
49. Brembeck P, Lorentzon M, Ohlsson C, Winkvist A, Augustin H. Changes in cortical volumetric bone mineral density and thickness, and trabecular thickness in lactating women postpartum. J Clin Endocrinol Metab. 2015; 100(2):535–43. [PubMed: 25387262]

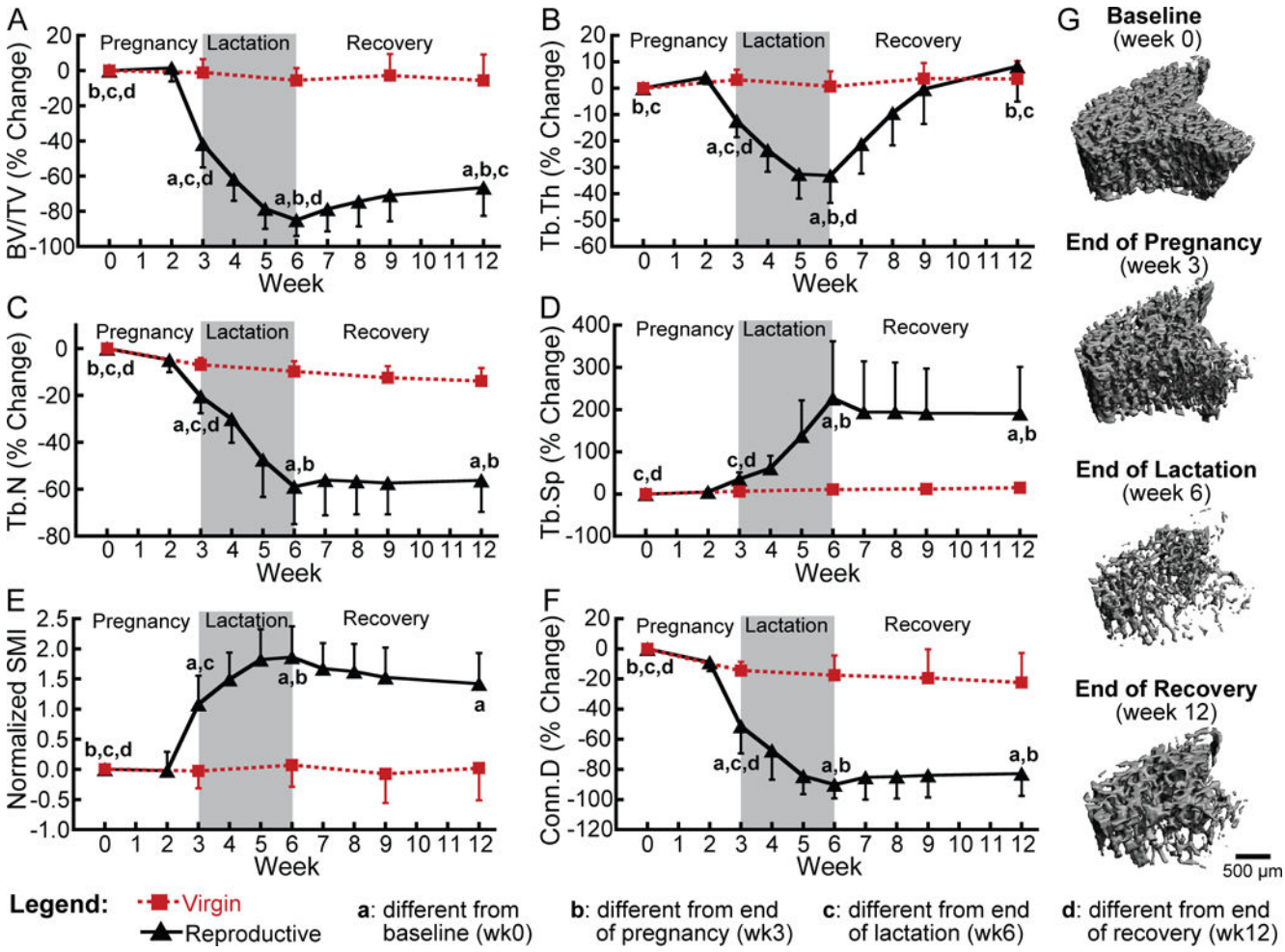

Figure 1.

(A–F) Changes in trabecular bone microarchitecture parameters throughout a reproductive cycle within the same trabecular VOI in reproductive rats (black triangles) and virgins (red squares). Letters indicate significant differences ($p<0.05$) among time points in the reproductive group (no significant changes over time were found for virgin rats). Intermediate time points (weeks 2, 4, 5, 7, 8, and 9) for virgin rats were not included in the analysis. (G) Representative 3D renderings illustrating changes in trabecular bone over the course of reproduction within a consistent trabecular VOI in a single rat.

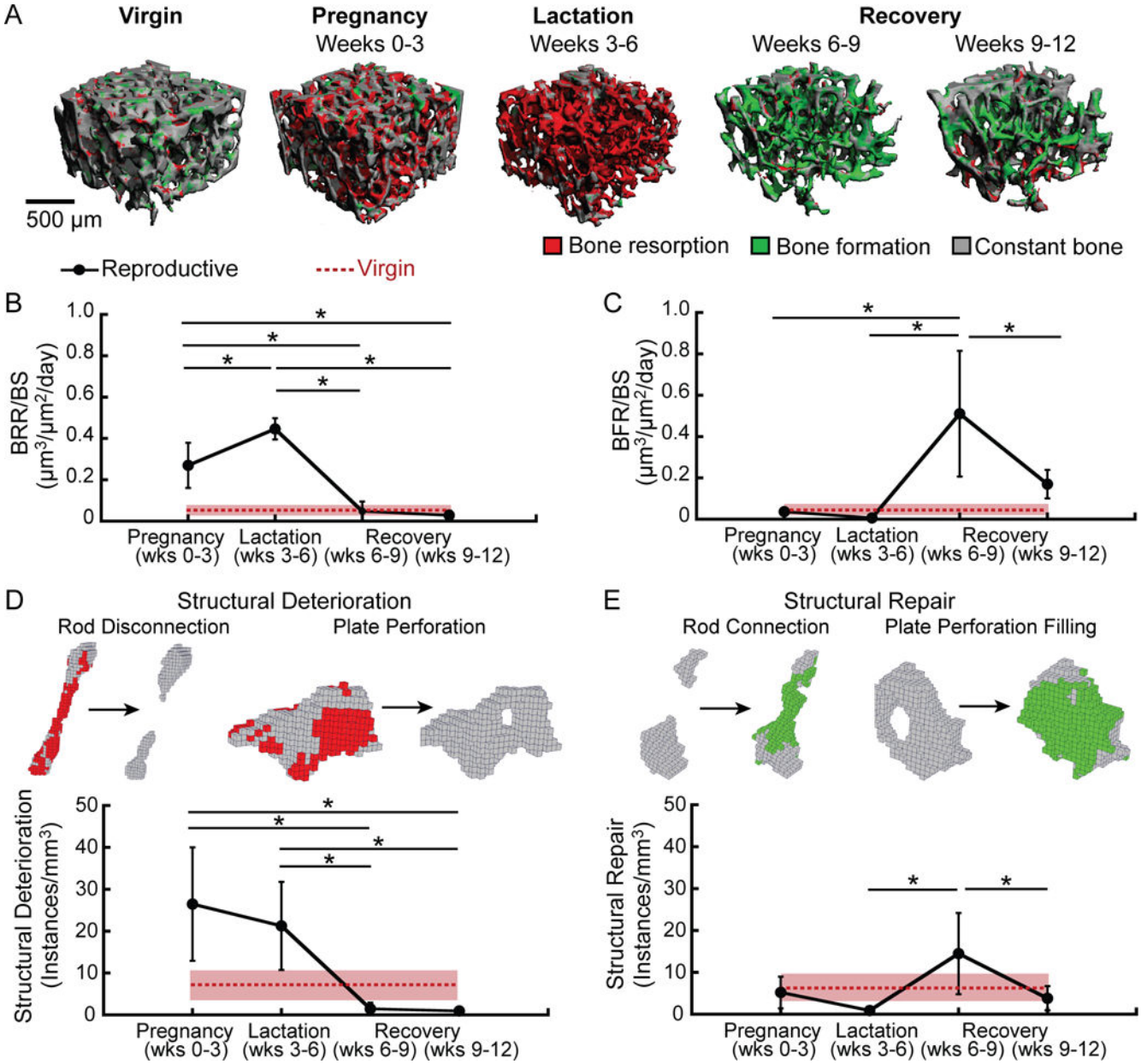

Figure 2.

(A) Representative 3D renderings illustrating bone (re)modeling (as determined by *in vivo* dynamic bone histomorphometry) over the course of pregnancy, lactation, and post-weaning recovery, as well as in virgin rats. Bone resorption (red) was highly elevated during pregnancy and lactation, while bone formation (green) was elevated post-weaning. Virgin rats showed low rates of bone (re)modeling, as indicated by the large amounts of constant bone (gray). (B) Bone resorption rate (BRR/BS), (C) bone formation rate (BFR/BS), (D) instances of structural deterioration, and (E) instances of structural repair over the course of 3 weeks of pregnancy, 3 weeks of lactation, and during two 3-week post-weaning recovery periods in reproductive rats (black dots and solid lines). Analogous measurements over a

single 3-week period are shown for virgin rats in red (dotted line; standard deviation shown in pink shading). *: significant difference between time points for reproductive rats ($p<0.05$).

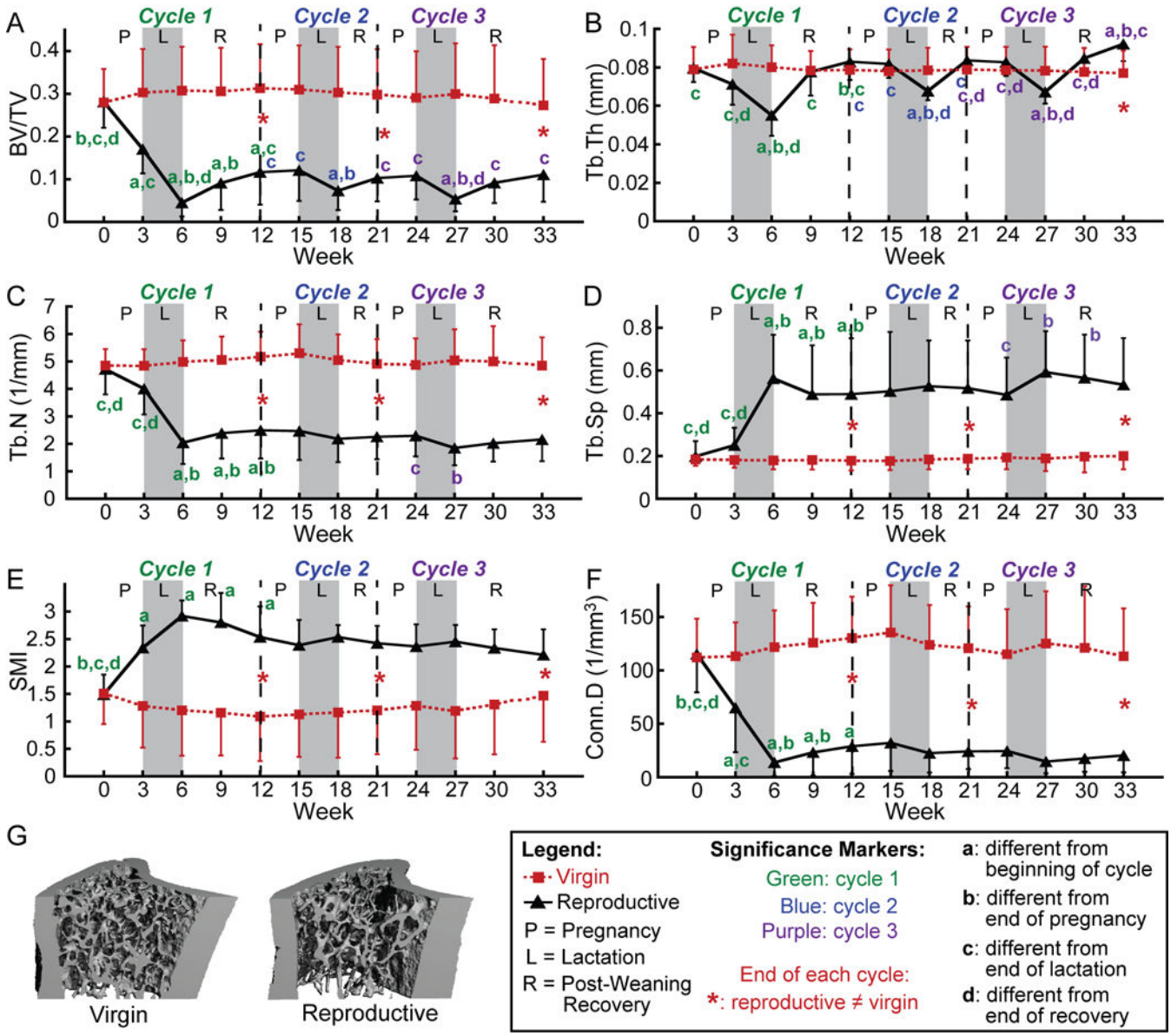

Figure 3.

(A–F) Changes in trabecular bone microarchitectural parameters over 3 cycles of pregnancy (P), lactation (L), and post-weaning recovery (R) in reproductive rats (indicated by black triangles) and virgins (represented by red squares). Letters indicate significant differences ($p<0.05$) among time points for each cycle in the reproductive group (no significant changes over time were found for virgin rats). Red * indicate differences between reproductive and virgin rats at the end of each cycle ($p<0.05$). (G) Representative 3D renderings of the proximal tibia of a virgin and reproductive rat at 3 months after the end of the last reproductive cycle.

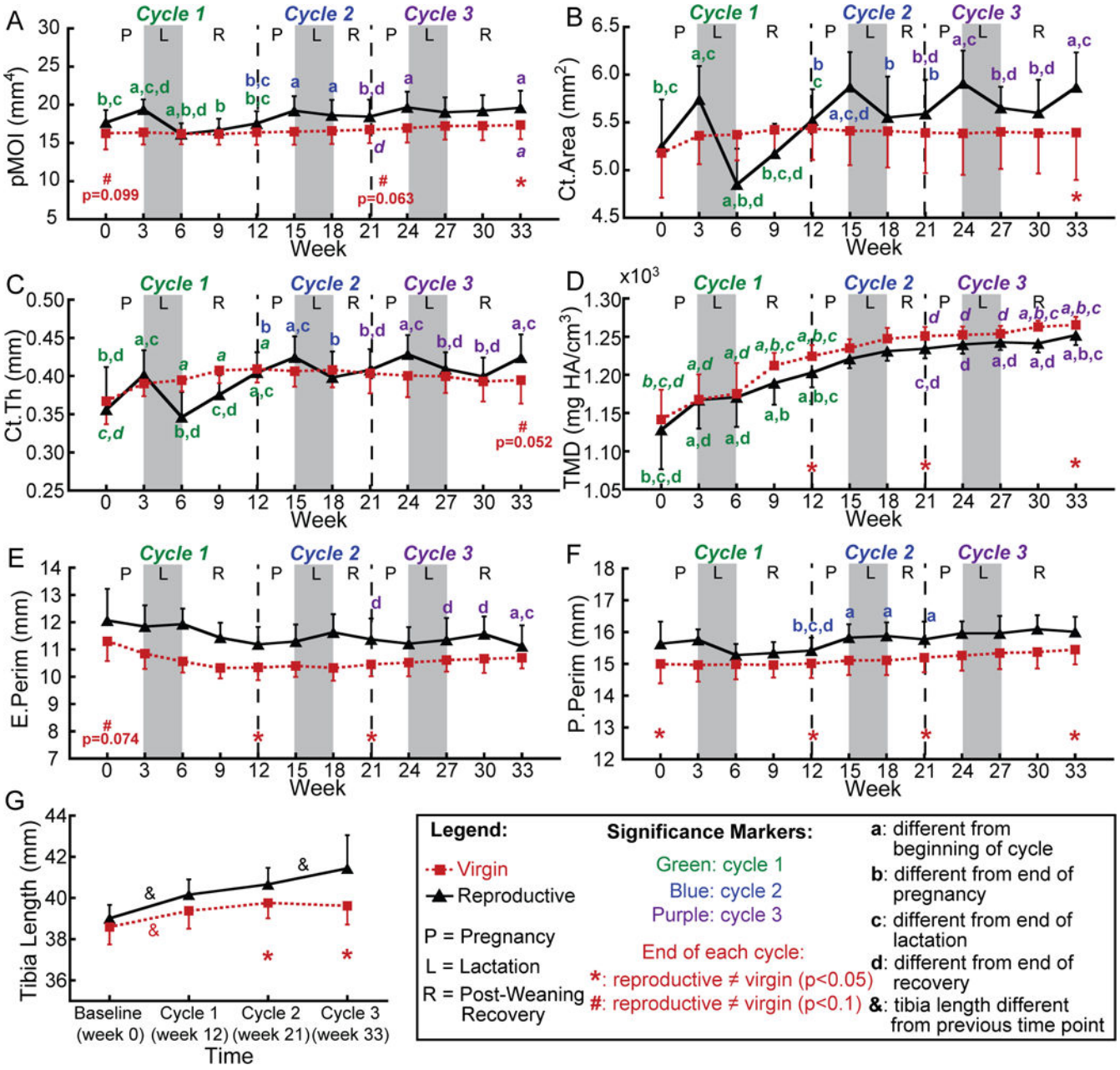

Figure 4.

(A–F) Changes in cortical bone structural parameters at the proximal tibia over 3 cycles of pregnancy (P), lactation (L), and post-weaning recovery (R) in reproductive rats (black triangles) and virgins (red squares). (G) Changes in total tibia length over 3 reproductive cycles. Letters indicate significant differences ($p<0.05$) in cortical parameters among time points for each cycle in the reproductive group (significant differences among time points in the control group are indicated by italic font), and & indicate significant differences in tibia length between consecutive reproductive cycles ($p<0.05$). Red * indicate differences between reproductive and virgin rats at the end of each cycle ($p<0.05$); red # indicate trends towards differences between reproductive and virgin rats at the end of each cycle ($p<0.1$).

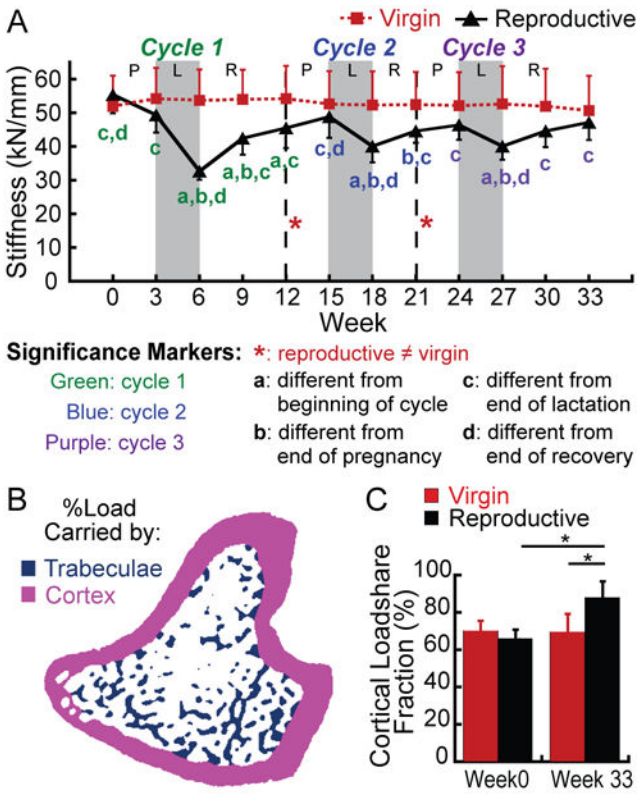

Figure 5.

(A) Changes in whole-bone stiffness at the proximal tibia over 3 cycles of pregnancy (P), lactation (L), and post-weaning recovery (R) in reproductive rats (black triangles), and virgins (red squares). Letters indicate significant differences ($p<0.05$) among time points for each cycle in the reproductive group (no significant changes over time were found for virgin rats). Red # indicates a trend towards a difference between reproductive and virgin rats at the end of the first reproductive cycle ($p<0.1$). (B) Schematic illustrating the separation of cortical (pink) and trabecular (blue) compartments in order to determine the percentage of the load carried by the trabecular and cortical bone (load-share fraction). (C) Percentage of load carried by the cortical bone at baseline and after 3 reproductive cycles in virgin and reproductive rats. *: $p<0.05$.